Mol Biotechnol (2015) 57:454–465
DOI 10.1007/s12033-015-9839-4

RESEARCH

Biochemical and Mutational Characterization of *N*-Succinyl-Amino Acid Racemase from *Geobacillus stearothermophilus* CECT49

Pablo Soriano-Maldonado · Montserrat Andújar-Sánchez · Josefa María Clemente-Jiménez · Felipe Rodríguez-Vico · Francisco Javier Las Heras-Vázquez · Sergio Martínez-Rodríguez

Published online: 21 January 2015

Abstract *N*-Succinyl-amino acid racemase (NSAAR), long referred to as *N*-acyl- or *N*-acetyl-amino acid racemase, is an enolase superfamily member whose biotechnological potential was discovered decades ago, due to its use in the industrial dynamic kinetic resolution methodology first known as "Acylase Process". In previous works, an extended and enhanced substrate spectrum of the NSAAR from *Geobacillus kaustophilus* CECT4264 toward different *N*-substituted amino acids was reported. In this work, we describe the cloning, purification, and characterization of the NSAAR from *Geobacillus stearothermophilus* CECT49 (GstNSAAR). The enzyme has been extensively characterized, showing a higher preference toward *N*-formyl-amino acids than to *N*-acetyl-amino acids, thus confirming that the use of the former substrates is more appropriate for a biotechnological application of the enzyme. The enzyme showed an apparent thermal denaturation midpoint of 77.0 ± 0.1 °C and an apparent molecular mass of 184 ± 5 kDa, suggesting a tetrameric species. Optimal parameters for the enzyme activity were pH 8.0 and 55–65 °C, with Co^{2+} as the most effective cofactor. Mutagenesis and binding experiments confirmed K166, D191, E216, D241, and K265 as key residues in the activity of GstNSAAR, but not indispensable for substrate binding.

Keywords *N*-Succinyl-amino acid racemase · *N*-Acyl-amino acid racemase · *N*-Acetyl-amino acid racemase · Acylase process · Amino acid · Racemase

P. Soriano-Maldonado · M. Andújar-Sánchez · J. M. Clemente-Jiménez · F. Rodríguez-Vico · F. J. Las Heras-Vázquez · S. Martínez-Rodríguez (✉)
Dpto. Química y Física, Universidad de Almería, Campus de Excelencia Internacional Agroalimentario, ceiA3, Edificio CITE I, Carretera de Sacramento s/n.,
04120 La Cañada de San Urbano, Almería, Spain
e-mail: srodrig@ual.es; sergio@ugr.es

P. Soriano-Maldonado · M. Andújar-Sánchez · J. M. Clemente-Jiménez · F. Rodríguez-Vico · F. J. Las Heras-Vázquez · S. Martínez-Rodríguez
Centro de Investigación en Biotecnología Agroalimentaria, BITAL, Almería, Spain

Present Address:
S. Martínez-Rodríguez
Department of Physical Chemistry, University of Granada, 18071 Granada, Spain

Introduction

N-Succinyl-amino acid racemase (NSAAR), long referred to as *N*-acyl- or *N*-acetyl-amino acid racemase (NAAR),[1] is an enolase superfamily member whose biotechnological potential was discovered decades ago, due to its use in the industrial dynamic kinetic resolution (DKR) methodology first known as "Acylase Process" [1]. Though this enzyme has been mainly studied because of its *N*-acetyl-amino acid racemase activity [1–9], its catalytic promiscuity attracted the attention of several scientists, whose work on the evolution and real classification of these enzymes [10–16] led them to propose its classification as a NSAAR [16, 17]. This enzyme belongs to the mechanistically diverse enolase superfamily, and in fact, it is an example of real catalytic promiscuity, since it is active toward many different substrates [10].

Despite a high number of patents describing the use of NSAAR/NAAR [18–24], and works related to the isolation

[1] We will use the three names indistinctly during this work, to try to maintain the original nomenclature used in the corresponding papers.

of microorganisms showing this activity [2, 25], only a small number of NSAAR/NAAR enzymes have been described in detail in the literature. In fact, only the enzymes belonging to *Amycolatopsis* [1–3, 6, 7, 26], *Deinococcus* [8, 27–30], *Streptomyces* [3], and *Geobacillus* [9, 16, 31–33] have been characterized to different extents. The crystallographic structure of *Thermus thermophilus* HB8 NAAAR has also been reported, but its activity has not been described [34]. Besides *N*-acetyl-amino acids, NSAAR/NAAR enzymes have also been reported to racemize other *N*-substituted amino acids to very different extents [3, 4, 6, 7, 9, 16, 32, 33, 35]. The recombinant NSAAR from *Geobacillus kaustophilus* CECT4264 (GkaNSAAR) proved to racemize *N*-formyl-amino acids more efficiently than the industrially used acyl-derivatives [31], allowing us to develop a more general and efficient DKR method based on the "Acylase Process" (namely Amidohydrolase Process) by coupling it with a stereospecific L-*N*-carbamoylase (Fig. 1) [32, 33]. Motivated by the potential of NSAAR enzymes in DKR processes for optically pure D- and L-amino acid production [28–30, 36], a recent paper highlights the efforts carried out by engineer improved NSAAR enzymes for this purpose [35]. Accordingly, it seems clear that finding new enzymes with improved characteristics or broader substrate spectrum would enhance this DKR methodology, since NSAAR enzymes constitute the limiting step for reaction in the bienzymatic tandems where this enzyme has been applied [28–30, 32, 33, 35].

In this work, we have cloned, overexpressed, purified, and characterized the NSAAR belonging to *Geobacillus stearothermophilus* CECT49 (GstNSAAR), specifically evaluating its *N*-formyl-amino acid racemase activity, since this activity has not been previously studied in detail for any NSAAR enzyme. In order to provide additional information on the mechanism and enzymatic features of NSAAR enzymes, we specifically altered five amino acids in the catalytic center of the enzyme to investigate their biochemical role in binding and catalysis.

Materials and Methods

Materials

All chemicals were of analytical grade and were used without further purification. Restriction enzymes and T4 DNA ligase were purchased from Roche Diagnostic S.L. (Barcelona, Spain). Kapa-Hifi polymerase was from Cultek S.L.U. (Madrid, Spain). Primers were from IDT (Biomol, Spain). TALON^{TM} metal affinity resin was purchased from Clontech Laboratories, Inc. Racemic and optically pure amino acids and *N*-acetyl-methionine were from Sigma Aldrich Quimica S.A. (Madrid, Spain). The *N*-carbamoyl-, *N*-succinyl-, and *N*-formyl-amino acids were synthesized according to previous works [9, 32, 33].

Microbes and Culture Conditions

Geobacillus stearothermophilus CECT49 *and Deinococcus radiodurans* CECT833 were used as possible donors of different *N*-succinyl-amino acid racemase (*nsaar*) genes. *Geobacillus stearothermophilus* CECT49 was grown on nutrient broth/agar I plates (1 % peptone, 0.5 % beef extract, 0.5 % NaCl, pH 7.2, 1.5 % Agar) at 55 °C (24 h). *Deinococcus radiodurans* CECT833 was grown on *Corynebacterium* broth/agar plates (1 % casein peptone (tryptic digest); 0.5 % yeast extract, 0.5 % glucose, 0.5 % NaCl, 1.5 % Agar) at 30 °C (72 h). *Escherichia coli* DH5α was used to clone the different putative *nsaar* genes, and *E. coli* BL21 (DE3) to overexpress the proteins.

Cloning of *N*-Succinyl-Amino Acid Racemase (*nsaar*) Genes

A single-colony isolate of *Geobacillus stearothermophilus* CECT49 and *Deinococcus radiodurans* CECT833 strains was chosen for DNA extraction by a boiling procedure. A sample of the supernatant containing genomic DNA (5 µl) was used to amplify the different fragments encoding for putative *nsaar* genes by PCR. Each of the obtained PCR fragments was purified from agarose gels using QIAquick (Qiagen) and then subcloned using a StrataClone^{TM} PCR Cloning Kit (Stratagene). The isolated sub-cloning plasmids were purified using QIAprep Spin miniprep kit (Qiagen), and digested using *Nde*I/*Xho*I (*Deinococcus radiodurans* CECT833 gene, *drcnsaar*) or *Sac*I/*BamH*I (*Geobacillus stearothermophilus* CECT49 gene, *gstnsaar*). The digested fragments were purified from agarose gel using QIAquick (Qiagen), and then the *drcnsaar* gene was ligated into *Nde*I/*Xho*I site of pET22b + plasmid (Novagen), and *gstnsaar* gene into the *Sac*I/*Bam*HI site of the rhamnose-inducible expression vector pJOE4036.1 [37]. The resulting constructions allowed the production of the *Geobacillus stearothermophilus* CECT49 NSAAR (GstNSAAR) and *Deinococcus radiodurans* CECT833 (DrcNSAAR) enzymes with a C-terminal His_6-tag. The cloned DNA fragments were sequenced using the dye dideoxy nucleotide sequencing method in an ABI 377 DNA Sequencer (Applied Biosystems). Translated sequences were aligned and compared with other available amino acid sequences using the Basic Local Alignment Search Tool (BLAST, NCBI). Clustal W-XXL was used for alignment [38].

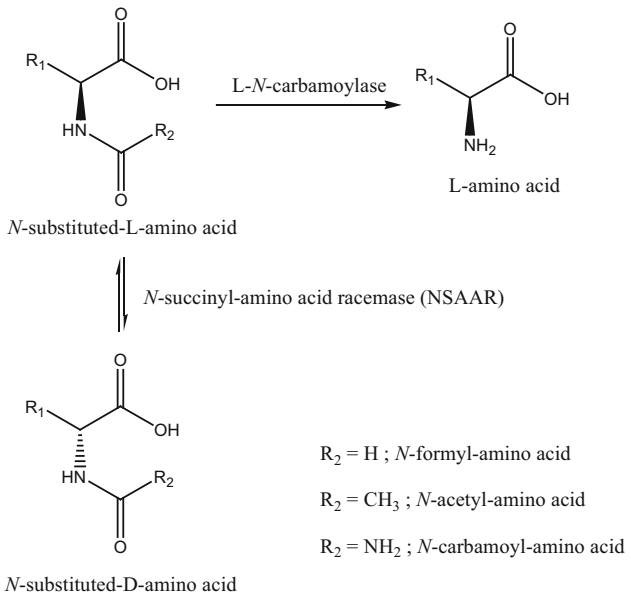

Fig. 1 Reaction scheme for optically pure L-amino acid production from racemic mixtures of *N*-substituted-amino acids using the "Amidohydrolase process". R_1 = lateral chain of the corresponding amino acid. R_2 = *N*-substituent. In the original "Acylase Process", $R_2 = CH_3$

Expression of GstNSAAR and DrcNSAAR

The different plasmids were transformed into *E. coli* BL21 (DE3) and then grown in LB medium supplemented with 100 μg/ml of ampicillin. A single colony was transferred into 10 ml of LB medium supplemented with 100 μg/ml of ampicillin in a 100-ml flask, and these cultures were incubated overnight at 37 °C with shaking. 500 ml of LB supplemented with 100 μg/ml of ampicillin were inoculated with 5 ml of the overnight culture in a 2-l flask. After 2 h of incubation at 37 °C with vigorous shaking, the OD_{600} of the resulting cultures was 0.3–0.5. For expression induction of the putative *gstnsaar* and *drcnsaar* genes, L-rhamnose (0.2 %) or isopropyl-β-thio-D-galactopyranoside (IPTG, 0.2 mM) was added to the cultures, respectively. The cultures were continued for a further 6 h at 32 and 34 °C, respectively. The cells were collected by centrifugation (Beckman JA2-21, 7,000 g, 4 °C, 20 min), and stored at −20 °C until use. Overexpression of GkaNSAAR enzyme was carried out as previously described [32].

Purification of GstNSAAR, DrcNSAAR, and GkaNSAAR Enzymes

Recombinant *E. coli* cells were resuspended in 30 ml wash buffer (300 mM NaCl, 0.02 % NaN_3, 50 mM sodium phosphate pH 7.0). The cell walls were disrupted in ice by sonication using a UP 200 S Ultrasonic Processor (Dr. Hielscher GmbH) for 6 periods of 30 s, pulse mode 0.5, and sonic power 60 %. The pellet was precipitated by centrifugation (Beckman JA2-21, 10,000*g*, 4 °C, 20 min) and discarded. The supernatant was applied to a column packed with cobalt metal affinity resin and then washed three times with wash buffer (see above). NSAAR enzymes were eluted with elution buffer (100 mM NaCl, 0.02 % NaN_3, 50 mM imidazole, 2 mM Tris, pH 8.0). Protein purity was determined at different stages of the purification by SDS-PAGE electrophoresis. An additional gel filtration chromatography step was carried out using a Superdex 200 gel filtration column (GE Healthcare) in a BioLogic Duo-Flow FPLC system (BioRad) to eliminate any DNA co-eluting with the protein, with observation at 280 nm. The purified enzyme was concentrated using an Amicon ultra-filtration system with Amicon YM-3 membranes, dialyzed against 100 mM Borate–HCl pH 8.0, and stored at 4 °C. Protein concentrations were determined from the absorbance of coefficient extinction of tyrosine residues [39].

Standard Enzymatic Assay

A standard enzymatic reaction was carried out to assess the activity of GstNSAAR, DrcNSAAR, and GkaNSAAR enzymes toward different *N*-substituted-amino acids. Purified enzymes (0.1–50 μM) were incubated together with different *N*-substituted-amino acids (15 mM), using 100 mM Borate/HCl buffer 1.6 mM $CoCl_2$ pH 8.0 (500 μl reaction volume). The reaction mixture was incubated at 45 °C, and aliquots of 75 μl were retrieved at different times and boiled at 95 °C for 5 min to stop the enzymatic reaction. Then, 675 μl of the corresponding mobile phase (see below) was added to the stopped sample before centrifugation (13,000 rpm, 10 min). Samples were analyzed in a HPLC system (LC2000Plus HPLC System, Jasco) equipped with a Chirobiotic T column (4.6 mm × 250 mm, ASTEC Inc., USA). The mobile phase was 70 % methanol, 30 % ammonium acetate (0.01 M), and 0.5 ml acetic acid per liter [33], pumped at a flow rate of 0.6 ml/min and measured at 200 nm. The specific activity of the enzymes was defined as the amount of enzyme that catalyzed the formation of 1 mmol of *N*-D- or *N*-L-substituted amino acid per min and mg of protein at 45 °C.

Characterization of GstNSAAR Enzyme

In order to get the apo-form of GstNSAAR, freshly purified enzyme (2.3 μM) was incubated overnight with 25 mM HQSA, followed by extensive dialysis in 100 mM Borate–HCl buffer pH 8.0. To analyze the effect of different cations on GstNSAAR activity, apo-GstNSAAR was incubated separately in the presence of 2 mM NaCl, KCl, LiCl,

CsCl, RbCl, $MgCl_2$, $CaCl_2$, $ZnCl_2$, $CoCl_2$, $NiCl_2$, $FeCl_2$, $PbCl_2$, and $HgCl_2$ in 100 mM Borate–HCl buffer pH 8.0 (final volume 20 µl) at 4 °C for 60 min, followed by the standard enzyme assay. The standard enzyme assay was used to determine optimum temperature and pH of GstNSAAR. The temperature range was 20–85 °C, and the buffers used were 100 mM sodium citrate (pH 4.0–6.0), 100 mM sodium phosphate (pH 6.0–8.0), 100 mM sodium Borate–HCl (pH 8.0–9.0), Tris–HCl (pH 7.5–9.0), and 100 mM Borate–NaOH (pH 9.0–10.5). Thermal stability of the enzyme (2.3 µM) in 100 mM Borate–HCl buffer pH 8.0 was determined after 60-min preincubation at different temperatures from 20 to 85 °C in the absence or presence (1.6 mM) of $CoCl_2$, followed by the standard activity assay. Kinetic studies of GstNSAAR were conducted using different *N*-formyl-D- and *N*-formyl-L-amino acids as substrate in 100 mM Borate–HCl buffer 1.6 mM $CoCl_2$ pH 8.0 following the standard assay, with concentrations of substrate up to 50 mM. The activity of GstNSAAR mutants was measured using the standard activity assay described above, increasing enzyme concentration up to 50 µM.

Alanine Scanning of GstNSAAR K166, D191, E216, D241, and K265

Mutagenesis was performed using QuikChange II Site-directed mutagenesis kit from Stratagene following the manufacturer's protocol, using the pET22b + plasmid containing GstNSAAR as template. Mutations were confirmed by using the dye dideoxy nucleotide sequencing method in an ABI 377 DNA Sequencer (Applied Biosystems). The plasmids containing the mutated residues (K166A, D191A, E216A, D241A, and K265A) were transformed into *E. coli* BL21 (DE3), and protein overexpression and purification were carried out as described above for the wild-type enzyme.

Circular Dichroism Experiments

The secondary structures of GstNSAAR mutants (K166A, D191A, E216A, D241A, and K265A) were compared to the wild-type GstNSAAR using far-UV circular dichroism (CD) spectra, recorded with a Jasco J850 CD spectrometer (Jasco Inc.) equipped with a JASCO PTC-423S/15 Peltier accessory. Experiments were acquired with a response time of 8 s, a bandwidth of 1, and a step resolution of 0.2 nm. Protein concentrations were 2–6 µM in 10 mM Borate–HCl buffer pH 8.0. CD measurements were taken at 25 °C using a 1-mm pathlength cuvette. Spectra were acquired from 250 to 190 nm at a scan rate of 50 nm/min, and averaged over 5 scans.

For thermal denaturation experiments, CD spectra were measured in 100 mM Borate–HCl buffer 1.6 mM $CoCl_2$ pH 8.0 at a protein concentration of 5 µM in a 0.1 mm cuvette. Thermal denaturation measurements were monitored by measuring the changes in ellipticity at 222 nm. Denaturation data were collected at a scan rate of 0.2 °C/min, and the temperature was increased from 25 to 95 °C.

Binding Experiments with GstNSAAR Mutants

Fluorescence emission spectra were measured at 25 °C using an FP-6500 spectrofluorimeter (Jasco Inc.) equipped with an ETC 273T Peltier accessory with the proper excitation and emission wavelengths, using a cell of 1 cm path length. Enzymes were excited at 280 nm in order to obtain the intrinsic fluorescence spectra. The binding of *N*-formyl-D- or *N*-formyl-L-methionine to alanine mutants of GstNSAAR was monitored using the decrease in fluorescence emission at 341 nm. Excitation and emission bandwidths were 3 nm. Fluorescence measurements were corrected for dilution.

The saturation fraction, Y, can be expressed as

$$Y = \frac{K[\text{Ligand}]}{1 + K[\text{Ligand}]} \quad (1)$$

where K is the characteristic microscopic association constant and [Ligand] is the free concentration of *N*-formyl-D- or *N*-formyl-L-methionine. The saturation fraction, Y, can be calculated as

$$Y = \frac{\Delta F_{\text{corr}}}{\Delta F_{\text{corr}}^{\max}} = \frac{F(\text{Ligand}) - F(0)}{F(\infty) - F(0)} \quad (2)$$

where $F(0)$, F(Ligand), and $F(\infty)$ are the corrected fluorescence intensities for the protein solution without ligand, at a concentration of ligand equal to *N*-formyl-D- or *N*-formyl-L-methionine and at saturating ligand concentration, respectively.

Results and Discussion

Sequence Analysis of GstNSAAR and DrcNSAAR

A BLASTn search with the nucleotide sequence of *Geobacillus stearothermophilus* CECT49 revealed 99 % identity with the locus tag GK0926 from *Geobacillus kaustophilus* HTA426 (GenBank acc. No BA000043, region 949470-950594; prot BAD75211.1) and 97 % identity with the previously isolated *N*-succinyl-amino acid racemase gene from *Geobacillus kaustophilus* CECT4264 (EU427322.1). On the other hand, the BLASTn search with the nucleotide sequence of *Deinococcus radiodurans* CECT833 NSAAR genes revealed 100 % identity with the locus tag DR_0044 from *Deinococcus radiodurans* R1 (GenBank acc. No AE000513, region 42775-43899; prot AAF09631.1). The translated sequences of both genes were

used to carry out a sequence alignment with the other NSAAR enzymes described in the literature for which the sequence is available (Fig. 2). As expected, the higher sequence identities of GstNSAAR and DrcNSAAR were found with those of the other NSAAR from the same genera (GstNSAAR and GkaNSAAR, 97.6 % seq. id.; DrcNSAAR and *Deinococcus radiodurans* CCRC 12827 (DraNSAAR, [8]); 98.7 % seq. id.). Similar results were

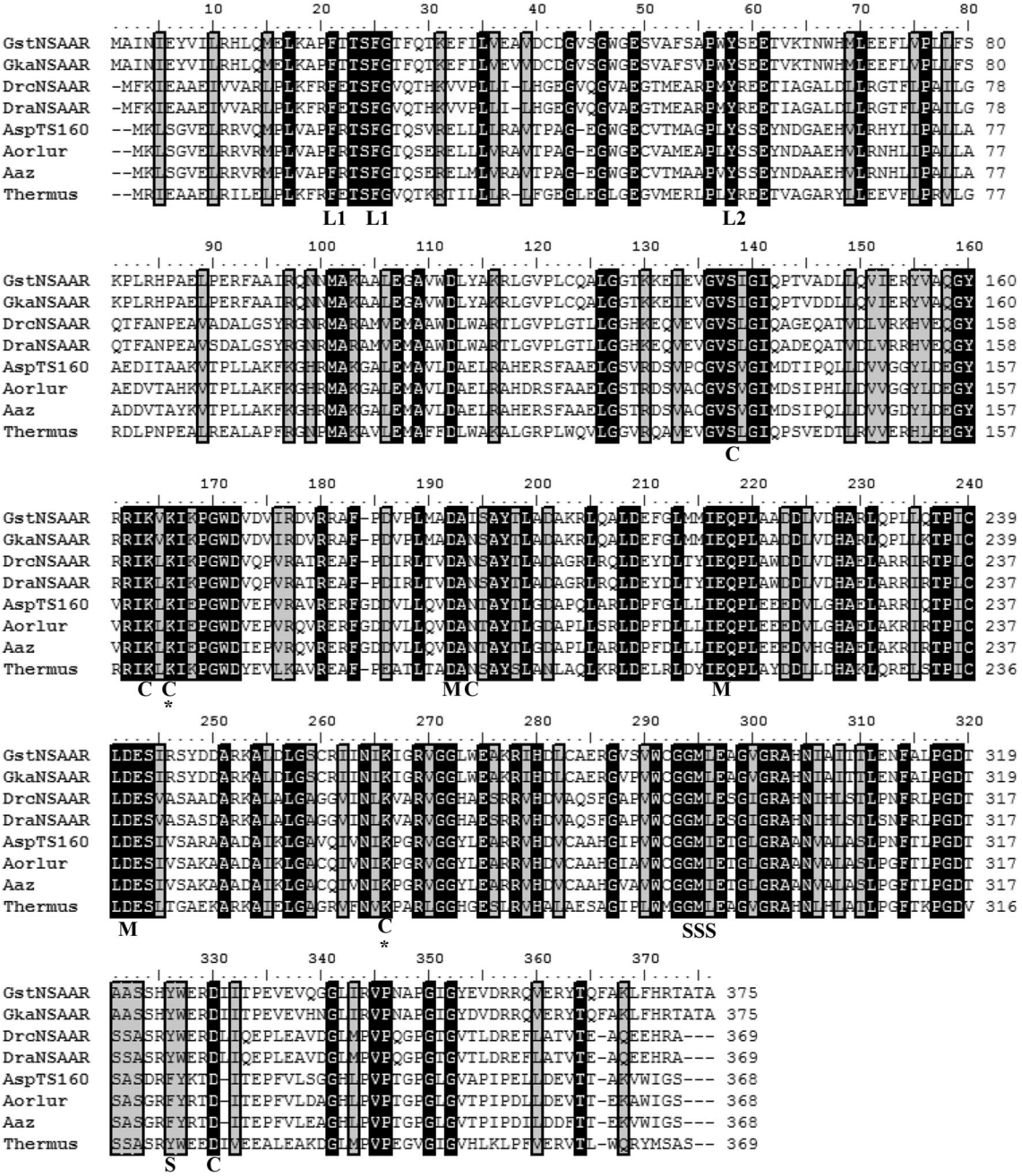

Fig. 2 Sequence alignment of the different NSAAR enzymes reported in the literature. GstNSAAR, NSAAR from *Geobacillus stearothermophilus* CECT49 (this work); GkaNSAAR, NSAAR from *Geobacillus kaustophilus* CECT4264, GenBank accession no. ABZ81711 [31]; DrcNSAAR, NSAAR from *Deinococcus radiodurans* CECT833 (this work); DraNSAAR, NSAAR from *Deinococcus radiodurans*, GenBank accession no. 1R0 M [8]; AspTS160, NSAAR from *Amycolatopsis* sp. TS-1-60, GenBank accession no. BAA06400 [4, 5]; Aorlur, NSAAR from *Amycolatopsis orientalis* subsp. *lurida*, GenBank accession no. CAC00653 [6]; Aaz, NSAAR from *Amycolatopsis azurea*, GenBank accession no. AF335269_1 [7]; Thermus, putative NSAAR from *Thermus thermophilus*, accession No BAD70697.1 [34]. The residues predicted to most likely configure the catalytic pocket of DraNSAAR are highly conserved among the different NSAAR above described, and are shown under the alignment with *letters* following the original nomenclature [8] (C: carboxyl group-binding site; M: metal-binding site; L1 and L2: L region; S: side-chain-binding region)

obtained with other NSAAR from the same genera (*Amycolatopsis orientalis* subsp. *lurida* and *Amycolatopsis azurea*; 95.1 % seq. id.). The *Geobacillus* and *Deinococcus* NSAARs shared a 47–48 % of seq. id. Sequence identities of GstNSAAR and DrcNSAAR with the other NSAAR from *Amycolaptosis* and *Thermus* were 42.8–48.5 and 43.6–59.7 %, respectively. A recent work already highlighted that NSAARs cannot be easily segregated into a family separate from the OSBS family, due to the high levels of sequence similarity and the bifunctionality shown by several of some OSBS/NSAAR family enzymes [40]. This fact would clearly explain why only the activity of NSAARs from five different microbial genera (see above) has been described in the literature (decreasing to three cases for which sequence–activity relationship has been proved; *Geobacillus*, *Deinococcus*, and *Amycolaptosis*). Eight subfamilies into the OSBS family of enzymes have been differentiated [40]; one of them is the so-called *Firmicutes* OSBS/NSAR subfamily, where the enzymes with proven NSAAR activity (*Geobacillus*, *Deinococcus* and *Amycolaptosis*) and that from *Thermus* are included. However, this subfamily also contains OSBS enzymes without NSAAR activity, such as *Bacillus subtilis* YtfD, sharing more than 40 % of sequence identity with NSAAR of proven activity [10]. Thus, a BLAST search strategy intended to look for new real NSAAR enzymes with potential biotechnological application might not be the most successful strategy, even if a high sequence identity cut-off is used, since as denoted above, sequences showing 40–50 % sequence identity do not always encode enzymes with NSAAR activity.

Expression and Purification of NSAAR Enzymes

Purification of GstNSAAR and DrcNSAAR enzymes yielded 5–20 mg of protein *per* liter of the recombinant *E. coli* culture. SDS-PAGE analysis indicated that the different enzymes were over 95 % pure after elution of the affinity column (Fig. 3), with an estimated molecular mass of 43 kDa (the deduced mass from the amino acid sequences, including the His_6-tag, is in the 43–44 kDa range). SEC-experiments conducted on a Superdex 200 10/300 column showed that GstNSAAR eluted at 15.2 mL (Fig. 3), corresponding to an apparent molecular mass of 184 ± 5 kDa. Since the theoretical molecular mass of a GstNSAAR tetramer is 174.3 kDa, our results suggest a tetrameric species (or a compacted higher-order oligomer). Similar results were obtained previously with GkaNSAAR (170–177 kDa) [31]. The NSAAR from *Streptomyces atratus* Y-53 (SatNSAAR) was described as an hexamer [3], whereas the enzymes belonging to *Amycolaptosis* [4, 6, 7] and *Deinococcus* [8] genera have been reported as octamers.

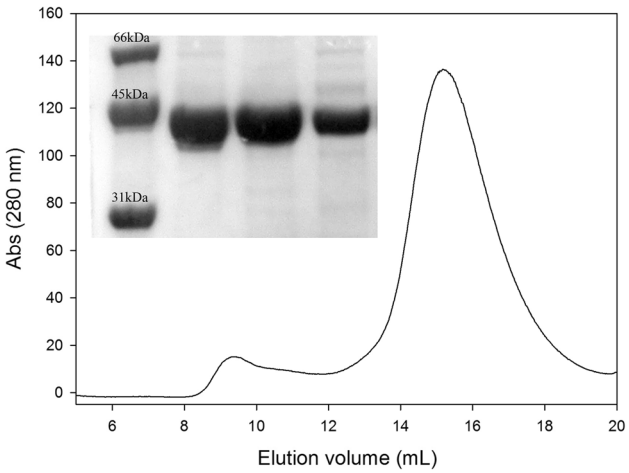

Fig. 3 Size exclusion chromatography elution profile of GstNSAAR using a Superdex 200 10/300 column. The *inset* represents the SDS-PAGE of the different purified recombinant NSAAR enzymes. *Lane 1*, low molecular weight marker; *lanes 2*, *3*, and *4*, purified GstNSAAR, GkaNSAAR, and DrcNSAAR, respectively

Table 1 Relative activity of GstNSAAR in the presence of different mono- and divalent cations, using the cobalt-amended GstNSAAR as reference

Sample	Relative activity (%)
apo-GstNSAAR	0.0 ± 0.0
Co^{2+}	100.0 ± 1.1
Ni^{2+}	55.8 ± 7.6
K^{+}	40.22 ± 8.4
Na^{+}	42.8 ± 10.4
Li^{+}	45.8 ± 5.4
Cs^{+}	47.8 ± 12.9
Rb^{+}	40.8 ± 8.5
Mg^{2+}	28.1 ± 2.9
Ca^{2+}	14.3 ± 0.7
Zn^{2+}	14.4 ± 6.5
Fe^{2+}	15.5 ± 0.6
Hg^{2+}	3.7 ± 4.0
Pb^{2+}	8.3 ± 0.9

The effect of the different cations was assayed using the apo-form of GstNSAAR. Values are the mean of three experiments, and the error indicates the standard deviation of the mean

Characterization of GstNSAAR Enzyme

Activity of GstNSAAR was assayed in the presence of different metal cations (Table 1). All the tested cations increased the activity of the apoenzyme, although cobalt exerted the highest increase. GstNSAAR enzyme was also active after IMAC purification (43.2 ± 0.4 % relative activity compared to the Co-amended enzyme), most likely

due to the NaCl present in the elution buffer, or even to Co^{2+} leakage from the IMAC column used for purification. Similar results have been shown with other NSAAR enzymes [3–9], although Mg^{2+} has been reported as the normal divalent metal ion utilized by members of the enolase superfamily [41]. Thus, all the characterization of GstNSAAR was carried out in the presence of this cofactor. GstNSAAR showed maximum activity at pH 8.0–8.5 and 55–65 °C. Similar results have been shown for other NSAAR enzymes ranging pHs 7.5–8.0 and 40–60 °C [3–9]. Thermal stability of GstNSAAR was studied by means of two techniques: (1) pre-incubating the enzyme in 100 mM Borate–HCl buffer pH 8.0 at different temperatures for 60 min, and subsequently measuring the residual activity; and (2) following the denaturation melting curve by means of far-UV CD. Activity was gradually lost when the enzyme was incubated in the absence of Co^{2+} at temperatures over 45 °C, and over 55 °C when Co^{2+} was present during the preincubation (Fig. 4). Similar results have been observed previously for GkaNSAAR, showing that the presence of the cation in the protein produces a stabilization of approximately 10 °C [31]. In view of this decrease in activity over 55 °C, we decided to carry out all subsequent reactions at 45 °C.

Although the thermal denaturation followed by far-UV CD (Fig. 4) was irreversible, and therefore, it was not possible to estimate the thermodynamic parameters governing thermal unfolding (ΔH_{vH}), we determined an apparent thermal denaturation midpoint ($T_{m(app)}$), as has been described for other proteins showing irreversible thermal denaturations [42, 43]. The $T_{m(app)}$ for GstNSAAR was 77.0 ± 0.1 °C (Table 3), confirming an apparent moderate thermostability of GstNSAAR, similar to that previously obtained with other NSAAR enzymes [9, 31]. The differences shown between the $T_{m(app)}$ and the midpoint calculated from the residual activity after preincubation (Fig. 4; approximately 15 °C) can be explained by the Equilibrium Model [44, 45]: enzymatic activity might be lowered or lost below the apparent unfolding temperature as a result of temperature-induced conformational changes at the active site from an optimum configuration for substrate binding to a less optimum one. Previous results with GkaNSAAR showing a different optimal temperature for *N*-formyl- and *N*-carbamoyl-amino acid racemization [32] also support temperature-induced conformational changes of the catalytic center.

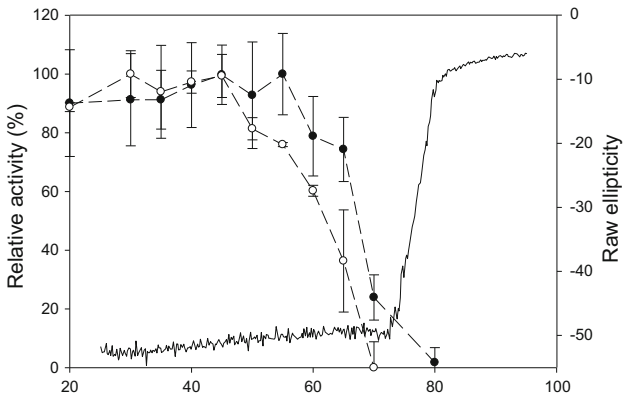

Fig. 4 CD-Thermal denaturation of cobalt-amended GstNSAAR followed by the changes in ellipticity at 222 nm (*continuous line*, *right axis*). The *plot* also shows the remaining relative activity of GstNSAAR after 60-min preincubation at the corresponding temperature, both in the presence (*filled circle*) and absence (*open circle*) of Co^{2+} (*left axis*). The results showing the remaining activity of GstNSAAR are the mean of three experiments, and the *error bars* indicate the standard deviation of the mean

Substrate Specificity of GstNSAAR

The major efforts on the activity characterization of NSAAR/NAAR enzymes have been focused on their *N*-acetyl-racemase activity. However, NSAAR/NAAR enzymes belonging to *Streptomyces*, *Amycolatopsis*, *Deinococcus,* and *Geobacillus* have also been reported to racemize to very different extents other *N*-substituted-amino acids such as *N*-propionyl-, *N*-butyryl-, *N*-benzoyl-, *N*-acetyl-, *N*-chloroacetyl-, *N*-carbamoyl-, *N*-succinyl-, and *N*-formyl-amino acids [3, 4, 6, 7, 9, 16, 32, 33, 35]. *Streptomyces* and *Amycolatopsis* NAARs are able to racemize *N*-formyl-amino acids (more slowly than the acylated species) [3, 4], but GkaNSAAR was the first NSAAR enzyme reported to racemize *N*-formyl-amino acids much faster than *N*-acetyl- or *N*-carbamoyl-amino acids [9]. In order to compare the catalytic properties of GstNSAAR and DrcNSAAR enzymes with those of previously characterized NSAAR enzymes, we also purified GkaNSAAR enzyme [9]. The enzymes were firstly confirmed to be active toward *N*-succinyl-D- and L-phenylalanine (Table 2). GstNSAAR and DrcNSAAR were also active to different degrees toward *N*-acetyl-, *N*-carbamoyl-, and *N*-formyl-amino acids (Table 2). Under the reaction conditions, GstNSAAR and GkaNSAAR were more efficient in all cases than DrcNSAAR (Table 2). Interestingly, although DraNSAAR has been mainly characterized and used for its *N*-acetyl- and *N*-carbamoyl-racemase activities [8, 29, 30, 34], our results show that DrcNSAAR racemizes *N*-formyl-methionine faster than the *N*-acetyl- and *N*-carbamoyl-derivatives, as observed with GstNSAAR and GkaNSAAR. Whereas GkaNSAAR has been the first NSAAR enzyme successfully used in the DKR of *N*-formyl-amino acids [32, 33], kinetic studies with *N*-formyl-amino acids had not been conducted previously [9]. Thus, kinetic parameters were obtained from hyperbolic saturation curves by least-squares fit of the data to the Michaelis–Menten equation (Fig. 5a). Reactions were carried out with

Table 2 Specific activities (μmol/min/mg of enzyme) of the different enzymes used in this work toward different *N*-substituted amino acids

	GKaNSAAR	GstNSAAR	DrcNSAAR
N-Succinyl-D-phenylalanine	3.3 ± 1.0	3.3 ± 0.2	2.4 ± 0.1
N-Succinyl-L-phenylalanine	7.9 ± 1.0	9.0 ± 0.2	4.5 ± 0.2
N-Formyl-D-methionine	4.7 ± 0.3	4.9 ± 0.5	2.6 ± 0.4
N-Acetyl-D-methionine	3.6 ± 0.0	3.7 ± 0.0	1.6 ± 0.0
N-Carbamoyl-D-methionine	0.7 ± 0.1	0.7 ± 0.1	0.3 ± 0.1
N-Formyl-D-norleucine	1.7 ± 0.3	1.9 ± 0.3	0.2 ± 0.0
N-Carbamoyl-D-norleucine	0.3 ± 0.0	0.3 ± 0.0	0.1 ± 0.0

Reaction conditions were the same in all cases for values to be comparable among them (15 mM substrate in 100 mM Borate–HCl 1.6 mM $CoCl_2$ pH 8.0, at 45 °C)

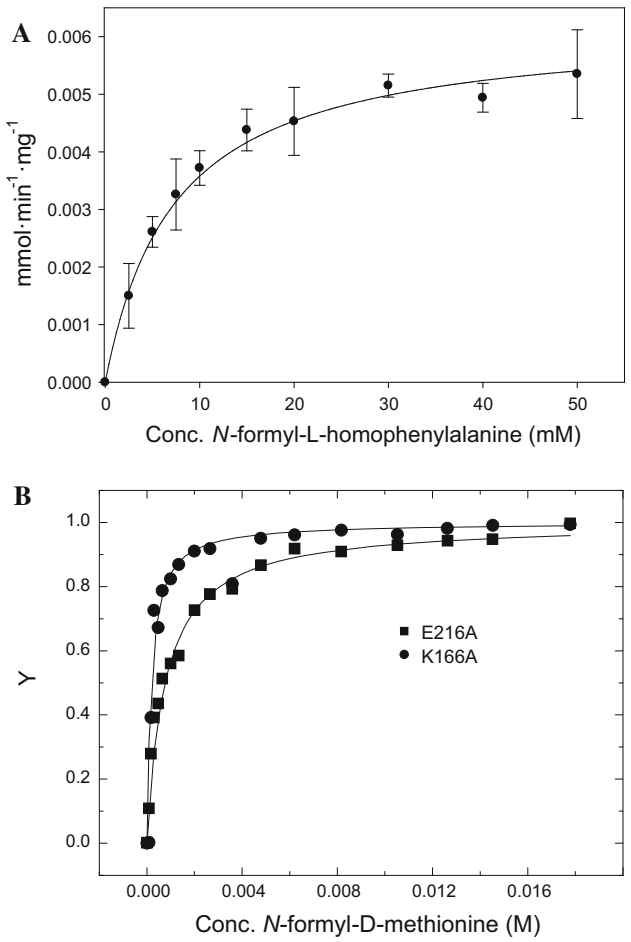

Fig. 5 **a** Kinetics of GstNSAAR using *N*-formyl-L-homophenylalanine as substrate (45 °C and pH 8.0). The results are the mean of three experiments, and the *error bars* indicate the standard deviation of the mean. **b** Fluorescence titration of *N*-formyl-D-methionine binding to E216A and K166A GstNSAAR mutants. Titrations were performed in 100 mM Borate–HCl buffer pH 8.0 and 25 °C, with enzyme concentrations in the range 0.81–0.95 μM. Stock ligand concentrations were 50 mM

different *N*-formyl-amino acids at varying concentrations (1–50 mM) at 45 °C and pH 8.0. The best substrate among those tested was *N*-formyl-homophenylalanine, with both the lowest K_m and highest k_{cat} values (Table 4). Taking into account the errors associated with the measurements, the first conclusion is that GstNSAAR presents a slightly higher catalytic efficiency toward the D-enantiomer of the substrates in most cases, similarly to the results observed previously with GkaNSAAR using *N*-acetyl-amino acids as substrates [9]. The k_{cat}/K_m values of GstNSAAR toward *N*-formyl-amino acids were in the 10^3–10^4/(M s) range (Table 4), whereas GkaNSAAR catalytic efficiency was in the 10–10^3/(M s) range with *N*-acetyl-amino acids [9]. Unexpectedly, the catalytic efficiency of GstNSAAR toward *N*-formyl-amino acids was in the same range than obtained for the natural substrates of *G. kaustophilus* HTA426 NSAAR [*N*-succinyl-amino acids; 10^3–10^4/(M s)] [16]. In fact, and whereas slightly lower, kinetic K_m and k_{cat} values of GstNSAAR toward *N*-formyl-L-methionine (9.0 ± 0.8 mM, 52.9 ± 1.4 s^{-1}) were very similar to those of *G. kaustophilus* HTA426 NSAAR with *N*-succinyl-L-methionine (3.6 ± 0.4 mM, 53.0 ± 1.0 s^{-1}) [16]. In *G. kaustophilus* HTA426, NSAAR appears in an operon together with highly enantioselective succinyl-CoA:D-amino acid *N*-succinyltransferase and *N*-succinyl-L-amino acid hydrolase enzymes, conforming a metabolic pathway for irreversible conversion of D-amino acids to their L-enantiomers [16, 17]. Despite the suggested moonlight character of NSAAR [16], based on the previous results on the isolated enzymes in the *G. kaustophilus* HTA426 "succinyl-transferase/racemase/hydrolase" operon (where less than 0.1 % of hydrolase activity was detected toward *N*-formyl-amino acids), the similar efficiency of GstNSAAR toward *N*-formyl- and *N*-succinyl-amino acids does not seem to support the former as an alternative natural substrate for this route.

When analyzing the *N*-formyl-amino acid racemization of GstNSAAR, GkaNSAAR, and DrcNSAAR, the catalytic efficiency values using *N*-formyl-D-norleucine were 1.9 ± 0.3, 1.7 ± 0.3, and 0.2 ± 0.0 s mM, respectively. Thus, *Geobacillus* enzymes presented an efficiency one order of magnitude higher than that of the *Deinococcus* enzyme, in accordance with the trend of the specific activities for the other *N*-substituted-amino acids (Table 2). Our results show that from a biotechnological point of view, even though DraNSAAR has been successfully applied in different DKR processes [29, 30, 34], GstNSAAR and GkaNSAAR enzymes might be better candidates for putative industrial applications based on their higher activities with the substrates assayed (Table 2).

Effect of Residues K166, D191, E216, D241, and K265 on the Activity of GstNSAAR

Previous mutagenesis studies carried out with *Amycolatopsis* sp T-1-160 NSAAR already concluded that NSAAR enzymes use a two-base mechanism for racemization, more specifically two lysine residues [13]. The crystallographic structure of this enzyme (PDB ID. 1SJA) showed three additional residues involved in substrate binding [14]. The five counterpart residues of GstNSAAR are K166, D191, E216, D241, and K265. We decided to mutate these residues to alanine in order to evaluate their implication in the activity and binding of GstNSAAR. Purity of the mutants was over 95 % (data not shown). Far-UV CD spectra were collected to evaluate the native-like folding of the Co-amended mutants. No significant differences were found in the far-UV CD spectra of the five alanine mutants, and we can therefore conclude that their secondary structure is basically the same as that of wild-type NSAAR (data not shown). Thermal melts were irreversible, as for the wild-type enzyme, but we determined the $T_{m(app)}$ values for all the mutants (Table 3). Since the temperature melts were irreversible, these values should be only considered as a qualitative measure of the similar stability of the WT and mutated species. Except for the thermal midpoint obtained for K265A mutant, which was higher than the rest, the melting curves, together with the steady-state far-UV data, suggest that the alanine scanning mutations did not alter significantly the native-like structure of the enzyme.

All the mutants showed negligible activity using up to 50 μM of enzyme (Table 3), confirming their key role in substrate racemization. Binding experiments with the alanine mutants using *N*-formyl-D- and *N*-formyl-L-methionine (Fig. 5b) yielded affinity constants in the range of 10^3–10^4 M^{-1} (Table 5), showing a slightly higher affinity for the D-enantiomer in all cases, and confirming these residues as not indispensable for *N*-formyl-amino acid binding despite its key role in the enzyme activity (Table 3). These results follow the same trend as the catalytic efficiency of the enzyme toward the different enantiomer pairs (Table 4), which also present a slight preference for the D-enantiomer. This slight preference agrees with the expected enantioselectivity of an NSAAR participating in the irreversible conversion of D-amino acids to their L-enantiomers using the above-mentioned "succinyl-transferase/racemase/hydrolase" operon [16]. Although the genome of *G. stearothermophilus* CECT49 is not available, the one from *G. stearothermophilus* str. 53 (GenBank Acc. No. JPYV01000018) also contains the counterpart operon, suggesting that this gene organization also might be present in *G. stearothermophilus* CECT49.

Since the $T_{m(app)}$ values for the three metal-binding mutants (D191A, E216A and D241A) were very similar to that found for the wild-type NSAAR (Table 3), we could argue that the three mutants are still able to bind the cation, since the presence of Co^{2+} produced a 10 °C increase in the thermal midpoint (see above). Whereas we cannot compare the affinity constants with those of the wild-type (they cannot be obtained as both isomers would be in solution), the affinity of the three mutants for both ligands decreased in the order D191A > D241A > E216A. By similarity of GstNSAAR and DraNSAAR (PDB ID 1XPY, [8]), the observed decrease in affinity might be a reflect of a lower polarization of the Co^{2+} cofactor by the absence of one of the carboxylate group of the lateral chains of the

Table 3 Thermal denaturation midpoints obtained for GstNSAAR and mutants in the presence of $CoCl_2$, and relative activities of the mutants using *N*-formyl-D- and *N*-formyl-L-methionine, compared to the wild-type enzyme

Enzyme	Thermal denat. midpoint (°C)	Relative activity (%) *N*-formyl-D-MET	Relative activity (%) *N*-formyl-L-MET
GstNSAAR	77.0 ± 0.1	100.00	100.00
K166A	78.5 ± 0.1	0.02	0.01
D191A	76.5 ± 0.1	0.00	0.02
E216A	78.7 ± 0.1	0.01	0.01
D241A	76.9 ± 0.1	0.01	0.02
K265A	83.4 ± 0.6	0.01	0.04

Table 4 Kinetic analyses of wild-type GstNSAAR

Substrate	K_m (mM)	k_{cat} (s^{-1})	k_{cat}/K_m/(s mM)
N-Formyl-D-methionine	12.6 ± 2.7	74.6 ± 5.1	5.9 ± 1.7
N-Formyl-L-methionine	9.0 ± 0.8	52.9 ± 1.4	5.9 ± 0.7
N-Formyl-D-norleucine	11.1 ± 4.1	12.3 ± 1.4	1.1 ± 0.5
N-Formyl-L-norleucine	12.5 ± 1.7	8.0 ± 0.4	0.6 ± 0.1
N-Formyl-D-aminobutyric acid	19.6 ± 3.7	15.2 ± 0.7	0.8 ± 0.2
N-Formyl-L-aminobutyric acid	17.9 ± 2.5	11.6 ± 0.7	0.7 ± 0.1
N-Formyl-D-norvaline	9.2 ± 1.8	11.2 ± 0.7	1.3 ± 0.3
N-Formyl-L-norvaline	24.5 ± 5.7	19.6 ± 1.4	0.8 ± 0.2
N-Formyl-D-homophenylalanine	3.0 ± 0.7	88.4 ± 4.3	29.5 ± 8.3
N-Formyl-L-homophenylalanine	5.7 ± 0.5	85.5 ± 0.7	15.0 ± 1.4

Kinetic parameters were obtained from hyperbolic saturation curves by least-squares fit of the data to the Michaelis–Menten equation. Reactions were carried out with the different *N*-formyl-amino acids at different concentrations (1–50 mM) at 45 °C and pH 8.0

three amino acids, altering the interaction of the cation with the carboxylate group of the substrate. However, this cation–carboxylate interaction is not totally indispensable for substrate binding, since we also confirmed that the three mutants are able to bind both enantiomers of the substrate, although with slightly lower affinity (data not shown). The absence of activity of the D191A, E216A, and D241A mutants (Table 3) also suggests that the proposed role of stabilization of the enediolate anion intermediate of the reaction by the cofactor is indispensable for the proposed two-base 1,1-proton transfer mechanism [8, 13]: mutation of any of the three-binding residues inactivates the enzyme, even when the cation is bound to the enzyme, hampering the racemization of the substrate.

The results with the K166A and K265A mutants are similar to those obtained previously for *Amycolatopsis* NSAAR [13]: mutation of these residues also inactivated GstNSAAR. These results are in accordance with the proposed two-base mechanism of the enolase superfamily [8, 13]. It is worth noting the apparent enhancement of K265A $T_{m(app)}$ (Table 3) and the apparent higher affinity of K166A toward *N*-formyl-D-methionine (Table 5). In the absence of additional results, we could only speculate on both interesting features. The homolog DraNSAAR X-ray structure (PDB ID 1XPY, [8]) shows that the counterpart lysine residues ($K168_{Dra}$ and $K269_{Dra}$) are situated 3.8 Å away from the cation. Since our results show that (i) the presence of the cation increases the GstNSAAR $T_{m(app)}$ and (ii) mutation in the metal-binding residues and the presence of the cation alter the affinity of GstNSAAR by the substrates (Table 5), we could argue that K166A and K265A mutations might produce alterations in the environment of the Co^{2+} cation, producing two different effects. In one hand, K265A mutation might result in a tighter binding of the cofactor, resulting in an even higher stabilization of the tertiary structure of GstNSAAR, thus increasing its $T_{m(app)}$. On the other hand, since the counterpart of K166 and D191 in the DraNSAAR structure ($K168_{Dra}$ and $D195_{Dra}$; PDB ID 1XPY, [8]) is positioned 2.8 Å away, we could argue that if K166–D191 interaction is lost due to the mutation, changes in the polarizability of the cation might occur, thus altering the affinity by the different ligands (Table 5).

Table 5 Binding constants obtained for *N*-formyl-D- and *N*-formyl-L-methionine GstNSAAR mutants

GstNSAAR mutant	Ligand	K (M^{-1})	Ratio D/L
K265A	*N*-Formyl-L-methionine	1,017 ± 22	1.7
	N-Formyl-D-methionine	1,689 ± 27	
D191A	*N*-Formyl-L-methionine	1,871 ± 18	1.2
	N-Formyl-D-methionine	2,195 ± 19	
D241A	*N*-Formyl-L-methionine	1,444 ± 12	1.4
	N-Formyl-D-methionine	2,024 ± 24	
E216A	*N*-Formyl-L-methionine	1,113 ± 39	1.2
	N-Formyl-D-methionine	1,343 ± 21	
K166A	*N*-Formyl-L-methionine	1,792 ± 33	2.9
	N-Formyl-D-methionine	5,269 ± 38	

Titration was performed at 25 °C in 100 mM Borate–HCl 1.6 mM $CoCl_2$ pH 8.0. Enzyme concentrations were in the range 0.8–1.0 μM and were titrated by addition of different ligand volume of solution at a concentration of 50 mM of *N*-formyl-D- or *N*-formyl-L-methionine

Conclusion

Several studies carried out by Glasneŕs group have previously highlighted two specific difficulties to find new NSAAR enzymes. Firstly, the high degree of similarity between the OSBS family [40] complicates the discovery of real NSAAR enzymes, since even members of the so-called *Firmicutes* NSAR/OSBS subfamily are not active toward *N*-succinyl-amino acids [10]. Secondly, several works have proven the difficulties to find the determinant allowing the evolution of OSBS family toward NSAAR activity [40, 46, 47]. The recent published studies on the role of the 20s loop of *Amycolatopsis* sp T-1-160 NSAAR [47] have shed some light on the importance of the conservation of not only the five residues mutated in this work, but also other residues previously observed in the substrate-bound crystallographic structure of DraNSAAR (Fig. 2) [8]. In our opinion, an alternative clue to find new biotechnologically relevant NSAAR enzymes/sequences, different to the only three for which a sequence–activity relationship has been proven (*Geobacillus, Deinococcus, Amycolaptosis*), might lie on the localization of similar *N*-succinyl-"transferase/racemase/hydrolase" operons similar to that reported previously [16].

Acknowledgments We thank Andy Taylor for critical discussion of the manuscript and Pedro Madrid-Romero for technical assistance. This work was supported by the Spanish Ministry of Education and Science, the European Social Fund (ESF), and the European Regional Development Fund (ERDF), through the project BIO2011-27842, by the Andalusian Regional Council of Innovation, Science and Technology, through the project TEP-4691, and by the European Cooperation in Science and Technology (COST) Action CM1303. P.S.-M. was supported by the University of Almería. S.M.-R. was supported by the Spanish Ministry of Science and Innovation.

References

1. May, O., Verseck, S., Bommarius, A., & Drauz, K. (2002). Development of dynamic kinetic resolution processes for biocatalytic production of natural and nonnatural L-amino acids. *Organic Process Research & Development, 6*, 452–457.
2. Tokuyama, S., Hatano, K., & Takahashi, T. (1994). Discovery of a novel enzyme, *N*-acylamino acid racemase in an actinomycete: Screening, isolation and identification. *Bioscience, Biotechnology, and Biochemistry, 58*, 24–27.
3. Tokuyama, S., Miya, H., Hatano, K., & Takahashi, T. (1994). Purification and properties of a novel enzyme, *N*-acylamino acid racemase, from *Streptomyces atratus* Y-53. *Applied Microbiology and Biotechnology, 40*, 835–840.
4. Tokuyama, S., & Hatano, K. (1995). Purification and properties of thermostable *N*-acylamino acid racemase from *Amycolatopsis* sp. TS-1-60. *Applied Microbiology and Biotechnology, 42*, 853–859.
5. Tokuyama, S., & Hatano, K. (1995). Cloning, DNA sequencing and heterologous expression of the gene for thermostable *N*-acylamino acid racemase from *Amycolatopsis* sp. TS-1-60 in *Escherichia coli*. *Applied Microbiology and Biotechnology, 42*, 884–889.
6. Verseck, S., Bommarius, A., & Kula, M. R. (2001). Screening, overexpression and characterization of an *N*-acylamino acid racemase from *Amycolatopsis orientalis* subsp. lurida. *Applied Microbiology and Biotechnology, 55*, 354–361.
7. Su, S.-C., & Lee, C.-Y. (2002). Cloning of the *N*-acylamino acid racemase gene from *Amycolatopsis azurea* and biochemical characterization of the gene product. *Enyzme and Microbial Technology, 30*, 647–655.
8. Wang, W. C., Chiu, W. C., Hsu, S. K., Wu, C. L., Chen, C. Y., Liu, J. S., & Hsu, W. H. (2004). Structural basis for catalytic racemization and substrate specificity of an *N*-acylamino acid racemase homologue from *Deinococcus radiodurans*. *Journal of Molecular Biology, 342*, 155–169.
9. Pozo-Dengra, J., Martinez-Gomez, A. I., Martinez-Rodriguez, S., Clemente-Jimenez, J. M., Rodriguez-Vico, F., & Las Heras-Vazquez, F. J. (2009). Racemization study on different *N*-acetylamino acids by a recombinant *N*-succinylamino acid racemase from *Geobacillus kaustophilus* CECT4264. *Process Biochemistry, 44*, 835–841.
10. Palmer, D. R., Garrett, J. B., Sharma, V., Meganathan, R., Babbitt, P. C., & Gerlt, J. A. (1999). Unexpected divergence of enzyme function and sequence: "*N*-acylamino acid racemase" is *o*-succinylbenzoate synthase. *Biochemistry, 38*, 4252–4258.
11. Thompson, T. B., Garrett, J. B., Taylor, E. A., Meganathan, R., Gerlt, J. A., & Rayment, I. (2000). Evolution of enzymatic activity in the enolase superfamily: Structure of *o*-succinylbenzoate synthase from *Escherichia coli* in complex with Mg^{2+} and *o*-succinylbenzoate. *Biochemistry, 39*, 10662–10676.
12. Schmidt, D. M., Hubbard, B. K., & Gerlt, J. A. (2001). Evolution of enzymatic activities in the enolase superfamily: Functional assignment of unknown proteins in *Bacillus subtilis* and *Escherichia coli* as L-Ala-D/L-Glu epimerases. *Biochemistry, 4051*, 15707–15715.
13. Taylor Ringia, E. A., Garrett, J. B., Thoden, J. B., Holden, H. M., Rayment, I., & Gerlt, J. A. (2004). Evolution of enzymatic activity in the enolase superfamily: Functional studies of the promiscuous *o*-succinylbenzoate synthase from *Amycolatopsis*. *Biochemistry, 43*, 224–229.
14. Thoden, J. B., Taylor Ringia, E. A., Garrett, J. B., Gerlt, J. A., Holden, H. M., & Rayment, I. (2004). Evolution of enzymatic activity in the enolase superfamily: Structural studies of the promiscuous *o*-succinylbenzoate synthase from *Amycolatopsis*. *Biochemistry, 43*, 5716–5727.
15. Glasner, M. E., Fayazmanesh, N., Chiang, R. A., Sakai, A., Jacobson, M. P., Gerlt, J. A., & Babbitt, P. C. (2006). Evolution of structure and function in the *o*-succinylbenzoate synthase/*N*-acylamino acid racemase family of the enolase superfamily. *Journal of Molecular Biology, 360*, 228–250.
16. Sakai, A., Xiang, D. F., Xu, C., Song, L., Yew, W. S., Raushel, F. M., & Gerlt, J. A. (2006). Evolution of enzymatic activities in the enolase superfamily: *N*-succinylamino acid racemase and a new pathway for the irreversible conversion of D- to L-amino acids. *Biochemistry, 45*, 4455–4462.
17. Song, L., Kalyanaraman, C., Fedorov, A. A., Fedorov, E. V., Glasner, M. E., Brown, S., et al. (2007). Prediction and assignment of function for a divergent *N*-succinyl amino acid racemase. *Nature Chemical Biology, 3*, 486–491.
18. Bommarius, A., Drauz, K., Kula, M.-R., & Verseck, S. (2001). *N*-Acetylamino acid racemase. EP 1074628 A1.
19. Bommarius, A., Drauz, K., Verseck, S., & Kula, M.-R. (2004). Acetyl amino acid racemase from *Amycolatopsis orientalis* for racemizing carbamoyl amino acids. US Patent 6767725 B2.
20. Bommarius, A., Drauz, K., & Verseck, S. (2008). Racemization and deprotection of special N-protected amino acids in the acylase/racemase system for the total conversion of special N-protected racemic amino acids into optically pure amino acids. US Patent 7378269 B2.

21. Verseck, S., Kula, M.-R, Bommarius, A., & Drauz, K. (2002). For producing enantiomer-enriched amino acids, and derivatives. US Patent 6372459 B1.
22. Takahashi, T., & Hatano, K. (1989). Acylamino acid racemase, Production and use thereof. EP 0304021 A2.
23. Takahashi, T., & Hatano, K. (1991). Acylamino acid racemase, production and use thereof. US Patent 4981799 A.
24. Tokuyama, M., Hatano, K., Nakahama, K., & Takahashi, T. (1992). DNA encoding acylamino acid racemase and its use. EP 0474965 A2.
25. Srivibool, R., Kurakami, K., Sukchotiratana, M., & Tokuyama, S. (2004). Coastal soil actinomycetes: Thermotolerant strains producing *N*-acylamino acid racemase. *Science Asia, 30*, 123–126.
26. Tokuyama, S., & Hatano, K. (1996). Overexpression of the gene for *N*-acylamino acid racemase from *Amycolatopsis* sp. TS-1-60 in *Escherichia coli* and continuous production of optically active methionine by a bioreactor. *Applied Microbiology and Biotechnology, 44*, 774–777.
27. Chiu, W. C., You, J. Y., Liu, J. S., Hsu, S. K., Hsu, W. H., Shih, C. H., et al. (2006). Structure–stability–activity relationship in covalently cross-linked *N*-carbamoyl-D-amino acid amidohydrolase and *N*-acylamino acid racemase. *Journal of Molecular Biology, 359*, 741–753.
28. Hsu, S. K., Lo, H. H., Kao, C. H., Lee, D. S., & Hsu, W. H. (2006). Enantioselective synthesis of L-homophenylalanine by whole cells of recombinant *Escherichia coli* expressing L-aminoacylase and *N*-acylamino acid racemase genes from *Deinococcus radiodurans* BCRC12827. *Biotechnology Progress, 22*, 1578–1584.
29. Hsu, S., Lo, H., Lin, W., Chen, I., Kao, C., & Hsu, W. (2007). Stereoselective synthesis of L-homophenylalanine using the carbamoylase method with in situ racemization via *N*-acylamino acid racemase. *Process Biochemistry, 42*, 856–862.
30. Yen, M.-C., Hsu, W.-H., & Lin, S.-C. (2010). Synthesis of L-homophenylalanine with immobilized enzymes. *Process Biochemistry, 45*, 667–674.
31. Pozo-Dengra, J., Martínez-Rodríguez, S., Contreras, L. M., Prieto, J., Andújar-Sánchez, M., Clemente-Jiménez, J. M., et al. (2009). Structure and conformational stability of a tetrameric thermostable *N*-succinylamino acid racemase. *Biopolymers, 91*, 757–772.
32. Soriano-Maldonado, P., Rodríguez-Alonso, M. J., Hernández-Cervantes, C., Rodríguez-García, I., Clemente-Jiménez, J. M., Rodríguez-Vico, F., et al. (2014). Amidohydrolase process: Expanding the use of L-*N*-carbamoylase/*N*-succinyl-amino acid racemase tandem for the production of different optically pure L-amino acids. *Process Biochemistry, 49*, 1281–1287.
33. Soriano-Maldonado, P., Las Heras-Vazquez, F.J., Clemente-Jimenez, J.M., Rodriguez-Vico, F., & Martínez-Rodríguez, S. (2014). Enzymatic dynamic kinetic resolution of racemic *N*-formyl- and *N*-carbamoyl-amino acids using immobilized L-*N*-carbamoylase and *N*-succinyl-amino acid racemase. Applied Microbiology and Biotechnology. doi:10.1007/s00253-014-5880-7.
34. Hayashida, M., Kim, S. H., Takeda, K., Hisano, T., & Miki, K. (2008). Crystal structure of *N*-acylamino acid racemase from *Thermus thermophilus* HB8. *Proteins, 71*, 519–523.
35. Baxter, S., Royer, S., Grogan, G., Brown, F., Holt-Tiffin, K. E., Taylor, I. N., et al. (2012). An improved racemase/acylase biotransformation for the preparation of enantiomerically pure amino acids. *Journal of the American Chemical Society, 134*, 19310–19313.
36. Martínez-Rodríguez, S., Martínez-Gómez, A. I., Rodríguez-Vico, F., Clemente-Jiménez, J. M., & Las Heras-Vázquez, F. J. (2010). *N*-Carbamoyl-D- and L-amino acid amidohydrolases: Characteristics and applications in biotechnological processes. *Applied Microbiology and Biotechnology, 85*, 441–458.
37. Stumpp, T., Wilms, B., & Altenbuchner, J. (2000). Ein neues, L-rhamnoseinduzierbares expressionssystem für *Escherichia coli*. *Biospektrum, 6*, 33–36.
38. Larkin, M. A., Blackshields, G., Brown, N. P., Chenna, R., McGettigan, P. A., McWilliam, H., et al. (2007). Clustal W and Clustal X version 2.0. *Bioinformatics, 23*, 2947–2948.
39. Gill, S. C., & von Hippel, P. H. (1989). Calculation of protein extinction coefficients from amino acid sequence data. *Analytical Biochemistry, 182*, 319–326.
40. Zhu, W. W., Wang, C., Jipp, J., Ferguson, L., Lucas, S. N., Hicks, M. A., & Glasner, M. E. (2012). Residues required for activity in *Escherichia coli o*-succinylbenzoate synthase (OSBS) are not conserved in all OSBS enzymes. *Biochemistry, 51*, 6171–6181.
41. Babbitt, P. C., Hasson, M. S., Wedekind, J. E., Palmer, D. R., Barrett, W. C., Reed, G. H., et al. (1996). The enolase superfamily: A general strategy for enzyme-catalyzed abstraction of the alpha-protons of carboxylic acids. *Biochemistry, 35*, 16489–16501.
42. Galisteo, M. L., Mateo, P. L., & Sánchez-Ruiz, J. M. (1991). Kinetic study on the irreversible thermal denaturation of yeast phosphoglycerate kinase. *Biochemistry, 30*, 2061–2066.
43. Martínez-Rodríguez, S., Encinar, J. A., Hurtado-Gómez, E., Prieto, J., Clemente-Jiménez, J. M., Las Heras-Vázquez, F. J., et al. (2009). Metal-triggered changes in the stability and secondary structure of a tetrameric dihydropyrimidinase: A biophysical characterization. *Biophysical Chemistry, 139*, 42–52.
44. Eisenthal, R., Peterson, M. E., Daniel, R. M., & Danson, M. J. (2006). The thermal behaviour of enzyme activity: Implications for biotechnology. *Trends in Biotechnology, 24*, 289–292.
45. Daniel, R. M., Peterson, M. E., Danson, M. J., Price, N. C., Kelly, S. M., Monk, C. R., et al. (2009). The molecular basis of the effect of temperature on enzyme activity. *Biochemical Journal, 425*, 3533–3560.
46. Odokonyero, D., Ragumani, S., Lopez, M. S., Bonanno, J. B., Ozerova, N. D., Woodard, D. R., et al. (2013). Divergent evolution of ligand binding in the *o*-succinylbenzoate synthase family. *Biochemistry, 52*, 7512–7521.
47. McMillan, A. W., Lopez, M. S., Zhu, M., Morse, B. C., Yeo, I. C., Amos, J., et al. (2014). Role of an active site loop in the promiscuous activities of *Amycolatopsis* sp. T-1-60 NSAR/OSBS. *Biochemistry, 53*, 4434–4444.